Kaskela, A., Nasibulin, A.G., Zavodchikova, M., Aitchison, B., Papadimitratos, A., Tian, Y., Zhu, Z., Jiang, H., Brown, D.P., Zakhidov, A., and Kauppinen, E.I., Aerosol synthesized SWCNT networks with tuneable conductivity and transparency by dry transfer technique, Nano Letters 10, 4349-4355 (2010). © 2010 American Chemical Society. Reprinted with permission from American Chemical Society.

NANO LETTERS

pubs.acs.org/NanoLett

Aerosol-Synthesized SWCNT Networks with Tunable Conductivity and Transparency by a Dry Transfer Technique

Antti Kaskela,[†] Albert G. Nasibulin,*[,†] Marina Y. Timmermans,[†,#] Brad Aitchison,[‡] Alexios Papadimitratos,[§] Ying Tian,[†] Zhen Zhu,[†] Hua Jiang,[†] David P. Brown,[‡] Anvar Zakhidov,[||] and Esko I. Kauppinen*[,†,⊥]

NanoMaterials Group, Department of Applied Physics and Center for New Materials, Aalto University, P.O. Box 15100, 00076 Espoo, Finland, Canatu Oy, Tekniikantie 21, FI-02150 Espoo, Finland, Solarno, Inc., 153 Hollywood Drive, Coppell, Texas 75019, NanoTech Institute, University of Texas at Dallas, Richardson, Texas 75083, and VTT Biotechnology, Biologinkuja 7, 02044 Espoo, Finland

ABSTRACT We demonstrate an aerosol CVD process to dry deposit large-area SWCNT networks with tunable conductivity and optical transmittance on a wide range of substrates including flexible polymers. These SWCNT networks can be chemically doped to reach a sheet resistance of as low as 110 Ω/□ at 90% optical transmittance. A wide application potential of these networks is demonstrated by fabricating SWCNT network-based devices such as a transparent capacitive touch sensors, thin-film transistors (TFTs), and bright organic light-emitting diodes (OLEDs).

KEYWORDS Carbon nanotube, thin film, ITO replacement, transparent electrode, OLED, transistor

Single-walled carbon nanotube (SWCNT) networks are promising for future electronics because of their unique optical and electrical properties.[1] Optically transparent conductive electrodes are one of the potential application areas,[2] as components of widely utilized electrical devices, such as thin displays and touch sensors. Currently used transparent metal oxides such as indium−tin oxide (ITO) have several drawbacks, including a high refractive index and haze, spectrally nonuniform optical transmission, limited flexibility, restricted chemical robustness, and a depleted raw material supply.[3,4] The application potential has induced significant research interest to develop both SWCNT network and other carbon nanostructured coating deposition methods and postprocessing methods. Several recent studies have demonstrated transparent carbon nanotube- or graphene-based electrodes with performance approaching ITO having a sheet resistance, R_s, of 280 Ω/□ at optical transmittance, $T = 80\%$,[5] 470 Ω/□ at $T = 87\%$,[6] and 220 Ω/□,[7] 170 Ω/□,[8] and 140 Ω/□[5] $T = 90\%$. These processes typically involve several time- and resource-consuming[9−12] and potentially detrimental[13,14] liquid purification and dispersion steps. We have developed an aerosol CVD-based deposition process that can eliminate liquid processing prior to deposition altogether and therefore decrease the process duration and process-induced damaging of the nanotubes.

SWCNTs were synthesized by the thermal decomposition of ferrocene vapor in a carbon monoxide (CO) atmosphere.[15] In this study, two synthesis reactors were used, one being a laboratory-scale reactor consisting of a ferrocene saturator, a water-cooled injector probe, and a heated tube furnace with variable maximum temperature from 800 to 1200 °C. A 300 cm^3/min flow of CO was passed through ferrocene powder. This provided the conditions for ferrocene vapor saturation of 0.8 Pa at room temperature. The growth chamber was an alumina tube (with an internal diameter of 22 mm and a length of 550 mm) inserted inside the tube furnace. The flow containing ferrocene vapor was then introduced directly into the high-temperature zone of the ceramic tube reactor through the water-cooled probe (water temperature of 25 °C) inserted 6.5 cm deep into the reactor. An additional CO flow of 100 cm^3/min was introduced into the reactor between the water-cooled probe and the reactor tube. The second synthesis reactor that was used in this work was a scaled-up version having a reaction tube of 150 mm in diameter and 1.5 m in length. It was operated at a total CO flow rate of 4 L/min and at a temperature of 880 °C. Ferrocene is thermally decomposed in a temperature gradient formed between the injector probe and the ambient reactor temperature. The decomposition leads to supersaturated conditions that result in iron nanoparticle formation.

* Corresponding authors. (A.G.N.) E-mail: albert.nasibulin@tkk.fi. Tel: +358 50 33 975 38. Fax: +358 9 2451 3517. (E.I.K.) E-mail: esko.kauppinen@tkk.fi. Tel: +358 40 50 980 64. Fax: +358 9 2451 3517.

† Aalto University.

‡ Canatu Oy.

§ Solarno, Inc.

|| University of Texas at Dallas.

⊥ VTT Biotechnology.

Previously published as Marina Y. Zavodchikova.

Received for review: 05/12/2010
Published on Web: 09/23/2010

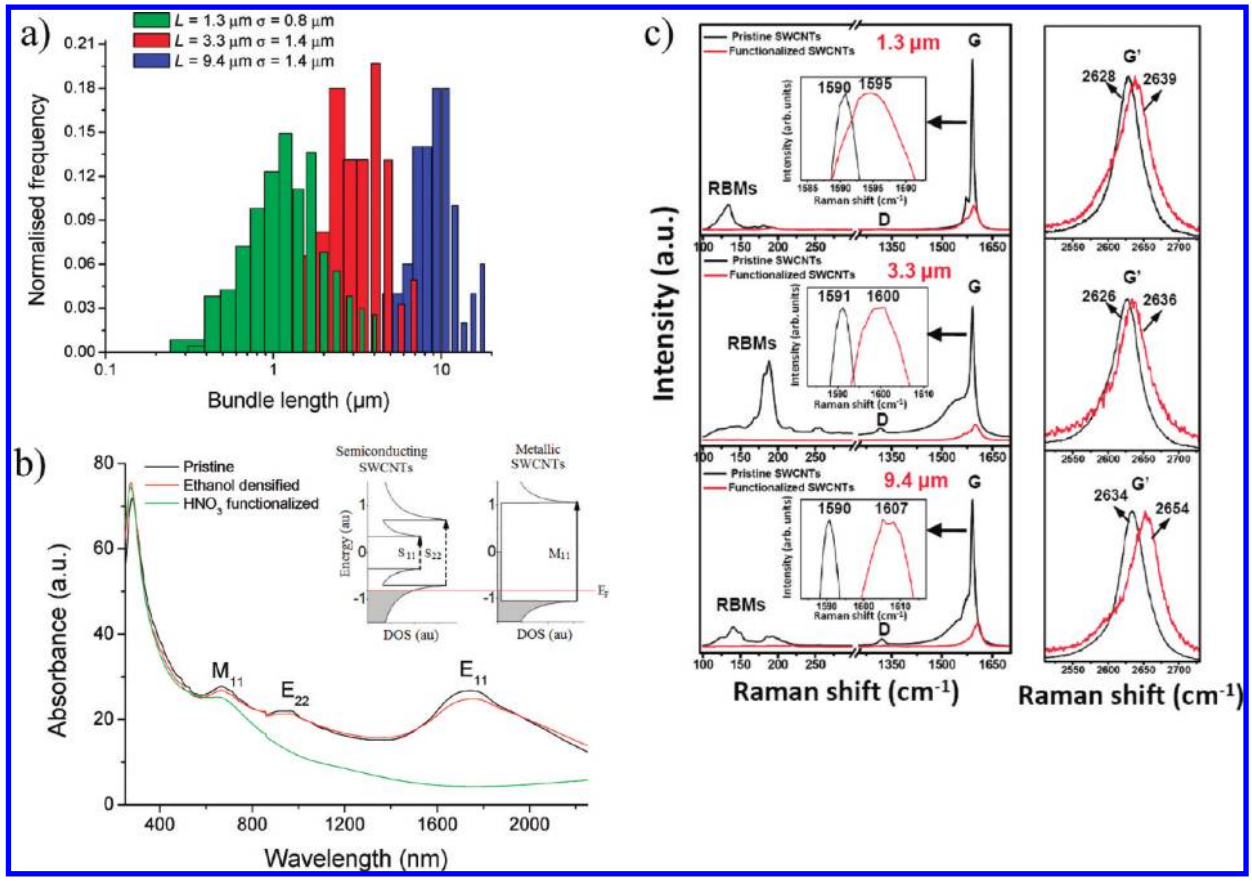

FIGURE 1. (a) Bundle length distribution of SWCNT samples used for the preparation of SWCNT films. Geometric mean bundle lengths are 1.3 ± 0.8, 3.3 ± 1.4, and 9.4 ± 1.4 μm. (b) Optical absorption spectra of a SWCNT network measured on a fused quartz substrate. Van Hove transitions S_{11} and S_{22} of semiconducting SWCNT and M_{11} of metallic SWCNTs are clearly visible, indicating the high quality of aerosol-CVD synthesized SWCNTs. The S_{11} and S_{22} transitions are not affected by ethanol densification but are completely suppressed after HNO_3 exposure because of the shift of the Fermi level, E_f, as a result of chemical doping as shown in the inset. (c) Raman spectra obtained from pristine and HNO_3-treated SWCNT networks. Postdeposition treatment with nitric acid significantly reduces the Raman signal intensity and results in the blue shift of the G (inset) and G′ bands, indicating doping of SWCNTs. The intensity of the G′ band was normalized to show the shift.

Carbon monoxide gas is decomposed on the formed iron catalyst particles, leading to SWCNT growth.

The electrical conductivity of a SWCNT network is limited by highly resistive junctions between SWCNT bundles.[17−19] Therefore, increasing the length of the SWCNT bundles is expected to decrease the network resistivity because of a smaller number of contacts in series. To study the effect of the SWCNT bundle dimensions on the electrical conductivity of the networks, we prepared samples with different bundle lengths of 1.3 ± 0.8, 3.3 ± 1.4, and 9.4 ± 1.4 μm as shown in Figure 1a. SWCNTs (1.3 and 3.3 μm long) were synthesized in the laboratory-scale ferrocene reactor. On the basis of in situ sampling experiments,[20] we have recently discovered that the length of the SWCNTs is determined by the reactor conditions and the SWCNT growth is terminated at temperatures higher than 945 °C. Therefore, to synthesize short SWCNT bundles (1.3 μm) we utilized a reactor temperature of 1050 °C where the SWCNT growth zone is limited. Longer SWCNT bundles with an average length of 3.3 μm were synthesized at lower temperatures (880 °C) to avoid the inhibition of the CO-disproportionation reaction and SWCNT growth termination. Bundles with an average length of 9.4 μm were synthesized with the scale-up reactor, which was designed to provide a longer residence time for the synthesis of longer SWCNTs. A 1% volumetric fraction of CO_2 was mixed at the inlet of the reactors to enhance the catalyst particle activity.[21] Bundle diameter distributions were found to be overlapping (Supporting Information, Figure S4). The bundle length and diameter characteristics were obtained by transmission and scanning electron microscopy (Philips CM200 FEG and JEOL JSM-7500F). SWCNT samples with submonolayer coverage were collected on TEM grids (holey carbon film 400 mesh CU, Agar Scientific, U.K.). The SWCNT network morphology was also studied by atomic force microscopy (Veeco Dimension 5000, Veeco Instruments).

The SWCNTs form small bundles in the gas phase, which were collected by a membrane filter at the outlet of the reactor to form a SWCNT network (Supporting Information, Figures S2 and S3). The sheet resistance and transmittance were controlled by the network deposition time and by the reactor dimensions and conditions.[16] The synthesized

DOI: 10.1021/nl101680s | Nano Lett. 2010, 10, 4349–4355

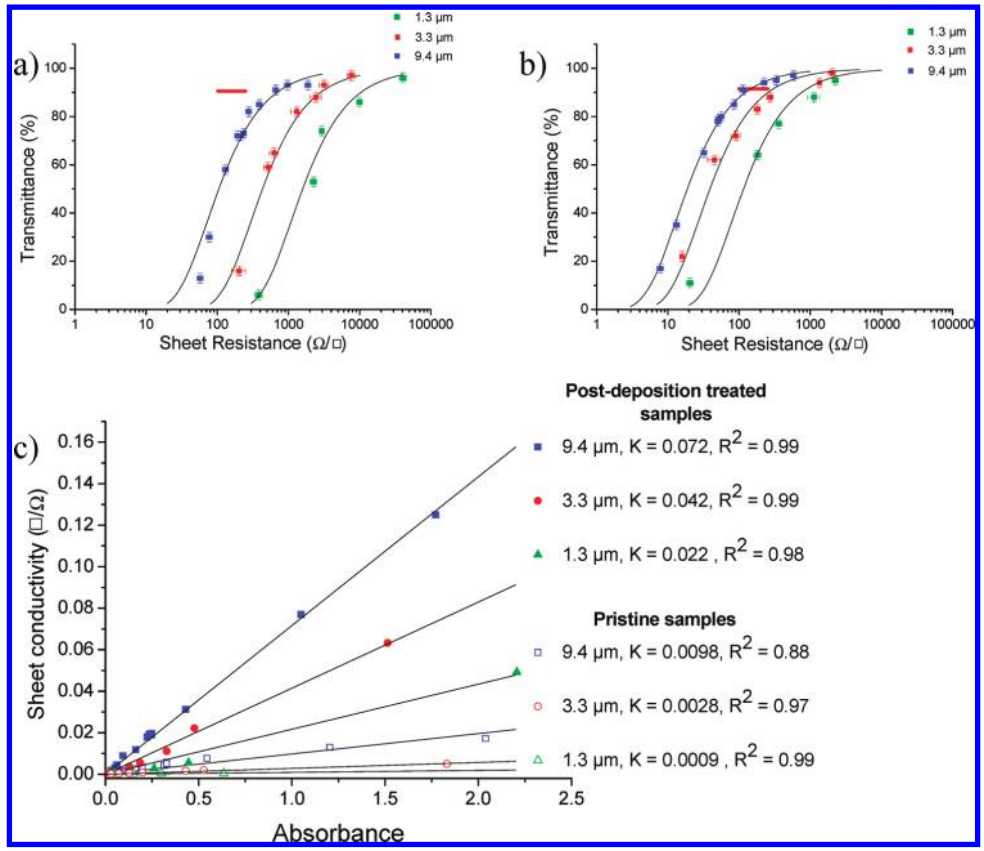

FIGURE 2. Sheet resistance versus optical transparency (at 550 nm) of (a) pristine and (b) HNO_3-treated SWCNT network electrodes. The optical transmittance can be tuned by varying the SWCNT network deposition duration. Solid lines shown are the approximated dependences between the sheet resistance and the optical transmittance. The range of sheet resistances of ITO-films on flexible substrates at $T = 90\%$ are indicated by a red mark. (c) Absorbance and sheet conductance relationship for SWCNT networks that are thicker than few monolayers. The linear relation can be obtained from Beer−Lambert's law whereas networks that are close to the percolation limit are described by percolation theory. The SWCNT network figure of merit, K, is dependent on the effective charge-carrier mobility and concentration (eq 6), which are integral functions of the properties of SWCNTs: their structural perfection, length of bundles, number of tube-to-tube contacts, interbundle junction resistance, degree of doping, and SWCNT network density (all factors that are controlled by the synthetic conditions or postdeposition treatment).

SWCNT bundles were collected downstream of the reactor by filtering the aerosol through a nitrocellulose membrane filter to form a SWCNT network (Millipore, HAWP, 0.45 μm pore diameter). The networks were transferred from a low adhesion filter to various substrates by a simple room-temperature press transfer process. Usable substrates range from flexible polymers (e.g., polyethylene terephthalate (PET)) to glass, quartz, silicon, and various metals (Supporting Information, Figure S4). A substrate and a SWCNT network on a filter were pressed together with a pressure of 10^3 Pa. No dispersion or purification steps were needed prior to the transfer, thus making the process of film preparation very rapid. The transfer process required less than 15 s to complete (Supporting Information, movie S1). Importantly, by utilizing masks beneath the filter, SWCNT network patterning can be achieved. Flexible electrodes of up to 28 × 28 cm^2 have been successfully fabricated by this method (Supporting Information, movie S2). Further scaling is possible by simply increasing the filter and substrate sizes. The press transfer method is compatible with roll-to-roll fabrication methods, thus opening up further upscaling potential in industrialized production. UV−vis−NIR optical absorption spectroscopy was performed using a dual-beam spectrophotometer (Lambda 950, Perkin-Elmer). A wavelength of 550 nm was used to characterize the optical transmittance of the films. The optical spectra of as-deposited SWCNTs reveal high-quality tubes (Figure 1b,c). The resistance was found to be strongly dependent on the average bundle length in the SWCNT network (Figure 2a). R_s of the sample containing the shortest bundles (1.3 μm) was 22 kΩ/□ at $T = 90\%$. The samples with longer bundles (3.3 and 9.4 μm) yielded SWCNT networks with $R_s = 2700$ and 820 Ω/□, respectively. The electrical sheet resistance of SWCNT networks was measured using a four-point linear probe and a multimeter (Jandel four-point probe, Jandel Engineering Ltd., England/Agilent 34411, Agilent) from five different locations on the SWCNT network.

To decrease the R_s of the SWCNT networks, we developed a fast postdeposition treatment. The SWCNT network was first densified by drop casting of ethanol and subsequent drying in a laboratory atmosphere. During evaporation, the surface tension of the ethanol compressed the network in

DOI: 10.1021/nl101680s | *Nano Lett.* **2010,** *10,* 4349–4355

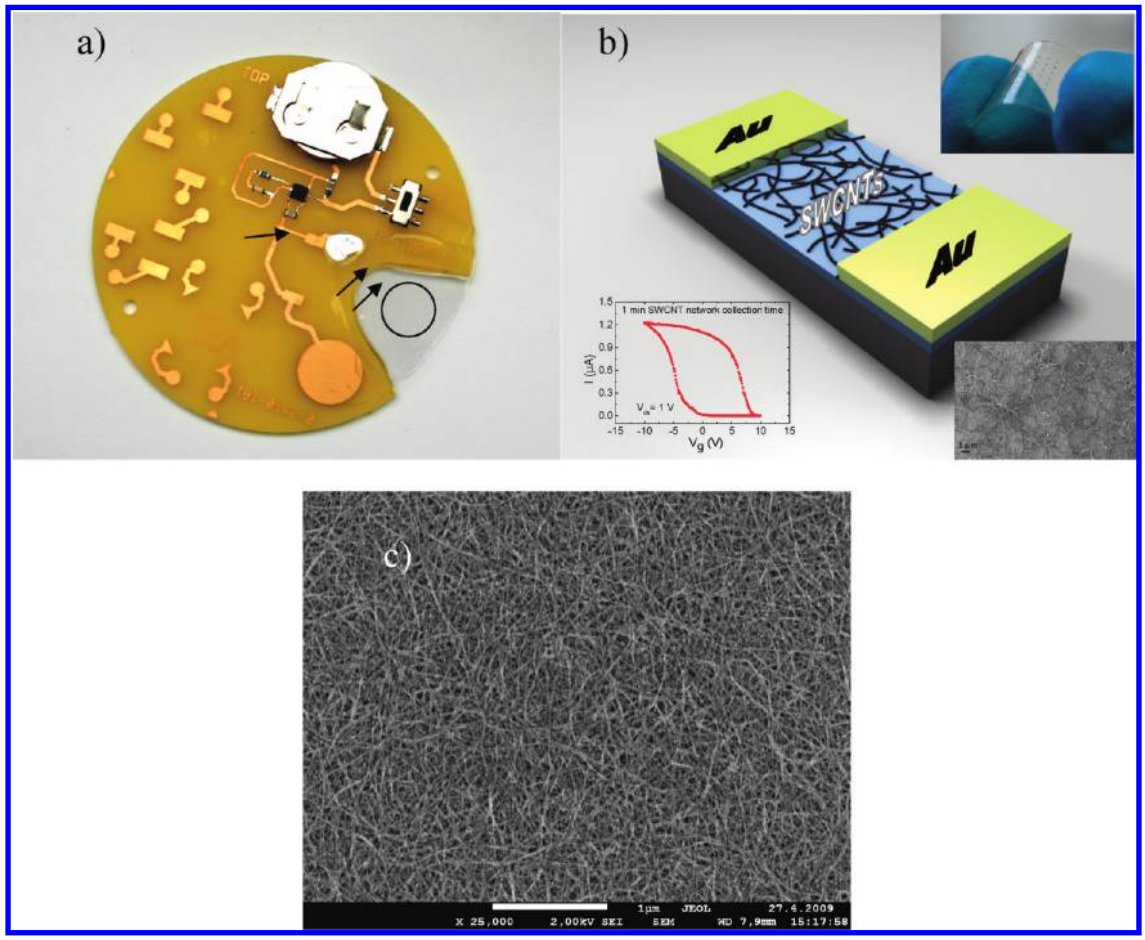

FIGURE 3. (a) Capacitive touch (proximity) sensor, which utilizes a highly transparent (98%, sheet resistance 4 kΩ/□) dry transferred SWCNT network as a sensing element (indicated by the circle). The SWCNT network covers the transparent PET substrate and also bridges the copper and SWCNT sensing element electrodes and the readout electronics (indicated by arrows), demonstrating the conductivity of the transparent film. (b) Schematics of a typical SWCNT network transistor. (Left inset) $I-V_g$ characteristics of a typical SWCNT network transistor, which was fabricated by dry transferring a SWCNT network below the metallic tube percolation threshold on the SiO_2-covered surface. (Upper right inset) Array of SWCNT TFTs on a flexible and transparent PET substrate. (c) SEM image showing the morphology of ethanol and a HNO_3-treated thick SWCNT electrode on a PET substrate.

the out-of-plane direction. This increased the network connectivity as the network morphology approached the 2-D limit, as can be observed from the SEM images (Supporting Information, Figure S3). The densification was followed by 60 s of dipping into concentrated HNO_3 and deionized water rinsing for 15 s to dope the semiconducting SWCNTs chemically and to decrease the interbundle junction resistance.[18] The morphology of the liquid-treated SWCNT network is shown in Figure 3b (and in Supporting Information, Figure S4). The improvement in SWCNT conductivity due to ethanol densification and HNO_3 treatment is depicted in Figure 2b. Importantly, SWCNT-network R_s dropped to as low as 110 Ω/□ at $T = 90\%$. For comparison, data for commercially available ITO films on flexible substrates are shown in Figure 2a,b.[22,23] The chemical treatment with HNO_3 has been demonstrated in previous studies, but with significantly longer treatment durations of 15 min, 60 min, and 3 h.[24−26] In our case, SWCNT films were doped within 1 min, which can be confirmed by optical absorption and Raman measurements. The electrical and optical characterizations were performed 1 h after the postdeposition treatment under ambient conditions. We used ethanol (Etax Aa, Altia, Finland) and 65% HNO_3 (65% HNO_3, J. T. Baker, Netherlands) in this study.

The suppression of optical transitions shown in Figure 1b suggests a shift in the Fermi level (Supporting Information, Figure S6). The charge transfer was confirmed by Raman spectroscopy. Raman measurements were performed using a 633 nm laser line (LabRAM, Horiba Yhoriba Jobin Yvon, France). We observed a significant decrease in Raman intensity and a blue shift in the G (inset of Figure 1c) and G′ bands (Figure 1c) in the acid-treated samples, indicating p-type doping of the SWCNTs (detailed discussion in Supporting Information).[27−29] This p-type doping decreases the resistance of the SWCNT network by enhancing the conduction of semiconducting tubes (Figure 2c).[26] According to Nirmalraj et al.,[18] the main role of the acid treatment should be attributed to a decrease in the interbundle junction resistance.

DOI: 10.1021/nl101680s | *Nano Lett.* **2010,** *10,* 4349–4355

It is worth noting that the electrical conductivity of SWCNT films thicker than a few monolayers can be described by bulk material conductivity laws. The thickness of the film, L, determines R_s (or sheet conductance, σ_s) to be

$$R_s = 1/\sigma_s = \rho_e a/(aL) = \rho_e/L = 1/(\sigma L) \quad (1)$$

where a is the side of a square sheet, ρ_e is the electrical resistivity, and σ is the electrical conductance, which can be calculated from

$$\sigma = en\mu \quad (2)$$

where e is the elementary charge, n is the charge-carrier concentration, and μ is the mobility. Optical absorption of the films can be described by the Beer−Lambert law. The absorbance, A, is proportional to the thickness of the film with a given density, ρ

$$A(\lambda) = -\ln(T(\lambda)) = \varepsilon(\lambda)\rho L \quad (3)$$

where $\varepsilon(\lambda)$ is a wavelength-dependent extinction coefficient. Usually electrical and optical properties of transparent conductive films are presented as σ_s versus T. By combining eqs 1−3, we obtain

$$R_s = -\frac{\varepsilon\rho}{enM \ln T} \quad (4)$$

Equation 4 can be linearized to get the relation between absorbance and sheet conductance

$$\sigma_s = KA \quad (5)$$

where

$$K = \frac{enM}{\varepsilon\rho} \quad (6)$$

is a coefficient of proportionality, which contains both optical and electrical characteristics of the film and can be used as a figure of merit to characterize the quality of SWCNT networks. For a certain type of SWCNTs (ε = const) with a certain density (ρ = const), the quality of the film will be determined by the concentration and mobility of the charge carriers. The concentration can be altered by the doping of SWCNTs, whereas the mobility in the network is determined by tube-to-tube contacts. Figure 2c demonstrates the method of comparing the relative performance of SWCNT networks with varying parameters by comparing their figure of merit (or coefficient of proportionality K).

Transparent SWCNT networks have several application areas where an easy dry transfer can be used to simplify and quicken device fabrication. We have built a capacitive touch (proximity) sensor from a highly (98%, sheet resistance 4 kΩ/□) transparent SWCNT network electrode on a PET substrate, which is connected to a PCB with read-out electronics (Supporting Information, Figure S1) and a touch indicator LED (QT100A, Amtel Corporation). The device is depicted in Figure 3a (Supporting Information, movie S3). The highly conductive SWCNT network coated area exhibits similar touch detection sensitivity to the copper electrode, and the SWCNT electrode can be contacted using silver paint with a low contact resistance of about 50 Ω. Press-transferred SWCNT networks with a density below the metallic percolation threshold can be used as a channel for the TFT. SWCNT networks with a 3.3 μm average bundle length were press-transferred onto a boron-doped Si substrate with a 100 nm SiO_2 gate dielectric. Source and drain electrodes were lithographically patterned on top of the SWCNT network, which was removed outside of the channel area by O_2 plasma etching (Supporting Information). Figure 3b shows the schematics of a SWCNT network transistor. The $I-V_g$ curve of a typical transistor with a low-density SWCNT network (1 min deposition) exhibiting an on/off ratio of 10^5 and mobility of ~3 $cm^2/(V\,s)$ is shown in the inset of Figure 3b and is estimated by using a parallel plate capacitance approximation. It is worth noting that mobility analysis by this approximation can significantly underestimate the mobility in cases where the gate dielectric is thin when compared to the tube separation, and in those cases, a more detailed analysis of gate capacitance coupling should be applied.[30] Higher-density networks (2 to 3 min deposition) exhibited mobility of over 20 $cm^2/(V\,s)$ but with reduced on/off ratios (Supporting Information, Figure S6). A semiconductor parameter analyzer (4155A, HP) was used for the electrical measurements of the SWCNT network transistors in air at room temperature. A similar dry-transfer technique was applied to the fabrication of TFTs on a flexible, transparent polymer material (inset in Figure 3a).

SWCNT networks are particularly convenient for applications in optoelectronic devices such as OLEDs. Figure 4 shows a schematic diagram of an OLED, actual light emission colors, current density versus voltage ($J-V$), luminance versus voltage ($L-V$) curves of low density, and highly transparent SWCNT sheets with different light-emitting materials. The active layers consisted of the following conjugated polymer materials: poly[9,9-dioctylfluorene] (PFO), poly[(9,9-dioctylfluorenyl-2,7-diyl)-*co*-(4,4-(*N*-(4-*sec*-butylphenyl))diphenylamine)] (TFB), and poly[2-methoxy-5-(2′-ethylhexyloxy)-1,4-phenylenevinylene] (MEH-PPV) (Supporting Information). The devices showed luminance of as high as 2000 cd/m^2 in the case of blue-emitting polyfluorene copoly-

DOI: 10.1021/nl101680s | *Nano Lett.* **2010,** *10,* 4349–4355

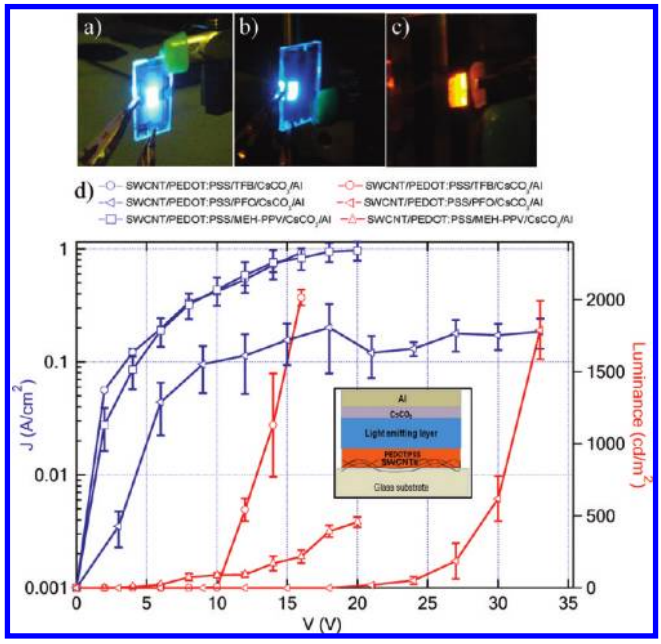

FIGURE 4. Bright OLEDs with highly transparent SWCNT anodes as effective hole injectors and various color light-emitting layers: (a) PFO with a thickness of 235 nm. (b) TFB with a thickness of 180 nm. (c) MEH-PPV with a thickness of 110 nm. (d) $I-V$ curves plotted together with luminance−voltage curves. The inset shows a schematic diagram of an OLED.

mers TFB and PFO. A significant advantage of the present SWCNT films deposited by the dry-transfer technique for OLEDs is that it allows the creation of very low density networks that cannot be easily made by any other technique including dry spinning from CVD forests.[31] Importantly, MWCNT sheets are not very flexible on small scales and may act mechanically as strong needles, which can electrically short through the thin emissive layer. The low-density SWCNT network was also found to be the most appropriate for the balanced injection of holes in OLEDs. Compared to brittle ITO, the extreme flexibility and high elasticity of SWCNT films open an avenue to a fully flexible OLED.

To conclude, we have demonstrated a fast, simple dry-transfer method of preparing SWCNT network films with easily tunable optical transparency and sheet resistance on various substrates. The method avoids liquid-based dispersion and purification steps, which are needed with traditional SWCNT film production techniques. Chemically doped SWCNT networks showed sheet resistance of as low as 110 Ω/□ at $T = 90\%$, which matches the typical ITO performance on flexible polymer substrates and to our knowledge is one of the lowest reported sheet resistances for SWCNT-based transparent electrodes. The sheet resistance of the SWCNT networks is found to be strongly dependent on the average bundle length of the produced SWCNTs. For films thicker than several monolayers, the optical transmittance and the electrical sheet resistance can be described by a simple phenomenological relation with an effective figure of merit K reflecting the properties of SWCNTs. The applicability of the dry-transfer method was demonstrated by applying it to fabricate optically transparent capacitive touch sensor electrodes, thin-film transistor channels, and OLED electrodes.

Acknowledgment. We thank Dr. A. S. Anisimov, Dr. K. Grigoras, Mr. Timo Murto, and Dr. Nikolay Houbenov for their assistance with experiments and Dr. I. S. Anoshkin, Dr. S. D. Shandakov, and Prof. Y. Ohno for fruitful discussions. This work was supported by the Academy of Finland (project nos. 128445 and 128495), TEKES, Aalto University through the Multidisciplinary Institute of Digitalization and Energy (MIDE) program and in part by the European Commission under the FP6 (STREP project BNC Tubes, contract NMP4-CT-2006-03350).

Supporting Information Available. Sample preparation. Flexibility demonstration. Capacitive touch sensor demonstration. Electron and atomic force microscopy characterization of SWCNTs. Examples of SWCNT deposits on various substrates. Postdeposition treatment of SWCNTs. SWCNT thin film transistor fabrication. Fabrication of bright OLEDs with SWCNT electrodes. Uniformity of the SWCNT electrodes and sample reproducibility. This material is available free of charge via the Internet at http://pubs.acs.org.

REFERENCES AND NOTES

(1) Wu, Z.; Chen, Z.; Du, X.; Logan, J. M.; Sippel, J.; Nikolau, M.; Karmaras, K.; Reynolds, J. R.; Tanner, D. B.; Hebard, A. F.; Rinzler, A. G. Transparent, conductive carbon nanotube films. *Science* **2004**, *305*, 1273–1276.
(2) Cao, Q.; Rogers, J. A. Ultrathin films of single-walled carbon nanotubes for electronics and sensors: a review of fundamental and applied aspects. *Adv. Mater.* **2008**, *21*, 29–53.
(3) Ke, L.; Kumar, R. S.; Chua, S. J.; Burden, A. P. Degradation study in flexible substrate organic light-emitting diodes. *Appl. Phys. A* **2005**, *81*, 969–974.
(4) Segal, M. Selling graphene by the ton. *Nat. Nanotechnol.* **2009**, *4*, 612–614.
(5) Kim, K. S.; Zhao, Y.; Jang, H.; Lee, S. Y.; Kim, J. M.; Kim, K. S.; Ahn, J.-H.; Kim, P.; Choi, J.-Y.; Hong, B. H. Large-scale pattern growth of graphene films for stretchable transparent electrodes. *Nature* **2009**, *457*, 706–710.
(6) Aguirre, C. M.; Auvray, S.; Pigeon, S.; Izquierdo, R.; Desjardins, P.; Martel, R. Carbon nanotube sheets as electrodes in organic light-emitting diodes. *Appl. Phys. Lett.* **2006**, *88*, 183104.
(7) Green, A. A.; Hersam, M. C. Processing and properties of highly enriched double-wall carbon nanotubes. *Nat. Nanotechnol.* **2008**, *4*, 64–70.
(8) Yim, J. H.; Kim, Y. S.; Koh, K. H.; Lee, S. Fabrication of transparent single wall carbon nanotube films with low sheet resistance. *J. Vac. Sci. Technol., B* **2008**, *26*, 851–855.
(9) Gruner, G. Carbon nanotube films for transparent and plastic electronics. *J. Mater. Chem.* **2006**, *16*, 3533–3539.
(10) Kaempgen, M.; Duesberg, G. S.; Roth, S. Transparent carbon nanotube coatings. *Appl. Surf. Sci.* **2005**, *252*, 425–429.
(11) Sreekumar, T. V.; Liu, T.; Kumar, S. Single-wall carbon nanotube films. *Chem. Mater.* **2003**, *15*, 175–178.
(12) Shin, J.; Shin, D. W.; Patole, S. P.; Lee, J. H.; Park, S. M.; Yoo, J. B. Smooth, transparent, conducting and flexible SWCNT films by filtration-wet transfer processes. *J. Phys. D: Appl. Phys.* **2009**, *42*, 45305–4309.
(13) Hecht, D. S.; Hu, L.; Gruner, G. Conductivity scaling with bundle length and diameter in single walled carbon nanotube networks. *Appl. Phys. Lett.* **2006**, *89*, 133112.
(14) Schrage, C.; Kaskel, S. Flexible and transparent SWCNT electrodes for alternating current electroluminescence devices. *ACS Appl. Mater. Interfaces* **2009**, *1*, 1640–1644.

DOI: 10.1021/nl101680s | *Nano Lett.* **2010,** *10,* 4349–4355

(15) Moisala, A.; Nasibulin, A. G.; Shandakov, S. D.; Jiang, H.; Kauppinen, E.I. Single-walled carbon nanotube synthesis using ferrocene and iron pentacarbonyl in a laminar flow reactor. *Chem. Eng. Sci.* **2006**, *61*, 4393–4402.
(16) Nasibulin, A. G.; Ollikainen, A.; Anisimov, A. S.; Pikhitsa, P. V.; Holopainen, S.; Penttilä, J. S.; Helistö, P.; Ruokolainen, J.; Choi, M.; Kauppinen, E. I. Integration of single-walled carbon nanotubes into polymer films by thermo-compression. *Chem. Eng. J.* **2008**, *136*, 409–413.
(17) Stadermann, M. Nanoscale study of conduction through carbon nanotube networks. *Phys. Rev. B* **2004**, *69*, 201402.
(18) Nirmalraj, P. N.; Lyons, P. E.; De, S.; Coleman, J. N.; Boland, J. J. Electrical connectivity in single-walled carbon nanotube networks. *Nano Lett.* **2009**, *9*, 3890–3895.
(19) Fuhrer, M. S.; Nygård, J.; Shih, L.; Forero, M.; Yoon, Y.-G.; Mazzoni, M. S. C.; Choi, H. J.; Ihm, J.; Louie, S. G.; Zettl, A.; McEuen., P. L. Crossed nanotube junctions. *Science* **2000**, *288*, 494–497.
(20) Anisimov, A. S.; Nasibulin, A. G.; Jiang, H.; Launois, P.; Cambedouzou, J.; Shandakov, S. D.; Kauppinen, E. I. Mechanistic investigations of single-walled carbon nanotube synthesis by ferrocene vapor decomposition in carbon monoxide. *Carbon* **2010**, *48*, 380–388.
(21) Nasibulin, A. G.; Brown, D. P.; Queipo, P.; Conzalez, D.; Jiang, H.; Kauppinen, E. I. An essential role of CO_2 and H_2O during single-walled CNT synthesis from carbon monoxide. *Chem. Phys. Lett.* **2005**, *417*, 179–184.
(22) Zhou, Y.; Zhang, F.; Tvingstedt, K.; Barrau, S.; Li, F.; Tian, W.; Inganäs, O. Investigation on polymer anode design for flexible polymer solar cells. *Appl. Phys. Lett.* **2008**, *92*, 233308.
(23) Wang, G.; Tao, X.; Wang, R. Flexible organic light-emitting diodes with a polymeric nanocomposite anode. *Nanotechnology* **2008**, *19*, 145201.
(24) Tangtan, H.; Ong, J. Y.; Loh, C. L.; Dong, X.; Chen, P.; Chen, Y.; Hu, X.; Tan, L. P.; Li, L.-J. Using oxidation to increase the electrical conductivity of carbon nanotube electrodes. *Carbon* **2009**, *47*, 1867–1885.
(25) Geng, H.; Kim, K. K.; So, K. P.; Lee, Y. S.; Chang, Y.; Lee, Y. H. Effect of acid treatment on carbon nanotube-based flexible transparent conducting films. *J. Am. Chem. Soc.* **2007**, *129*, 7758–7759.
(26) Parekh, B. B.; Fanchini, G.; Eda, G.; Chhowalla, M. Improved conductivity of transparent single-wall carbon nanotube thin films via stable postdeposition functionalization. *Appl. Phys. Lett.* **2007**, *90*, 121913.
(27) Lee, R. S.; Kim, H. J.; Fischer, J. E.; Thess, A.; Smalley, R. E. Conductivity enhancement in single-walled carbon nanotube bundles doped with K and Br. *Nature* **1997**, *388*, 255–257.
(28) Geng, H.-Z.; Kim, K. K.; Song, C.; Xuyen, N. T.; Kim, S. M.; Park, K. A.; Lee, D. S.; An, K. H.; Lee, Y. S.; Chang, Y.; Lee, Y. J.; Choi, J. Y.; Denayad, A.; Lee, Y. H. Doping and de-doping of carbon nanotube transparent conducting films by dispersant and chemical treatment. *J. Mater. Chem.* **2008**, *18*, 1261.
(29) Shin, D.-W.; Lee, J. H.; Kim, Y.-H.; Yu, S. M.; Park, S.-Y.; Yoo, J.-B. A role of HNO_3 on transparent conducting film with single-walled carbon nanotubes. *Nanotechnology* **2009**, *20*, 475703.
(30) Cao, Q.; Xia, M.; Kocabas, C.; Shim, M.; Rogers, J. A.; Rotkin, S. V. Gate capacitance coupling of single-walled carbon nanotube thin-film transistors. *Appl. Phys. Lett.* **2007**, *90*, No. 023516.
(31) Williams, C. D.; Robles, R. O.; Zhang, M.; Lee, S.; Baughman, R. H.; Zakhidov, A. A. Multiwalled carbon nanotube sheets as transparent electrodes in high brightness organic light-emitting diodes. *Appl. Phys. Lett.* **2008**, *93*, 183506.

DOI: 10.1021/nl101680s | *Nano Lett.* **2010,** *10,* 4349–-4355